

*1*  
*1970*

**KERNFORSCHUNGSZENTRUM  
KARLSRUHE**

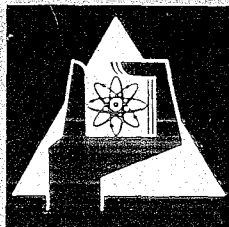
März 1970

KFK 1154  
IAEA-SM-130/38

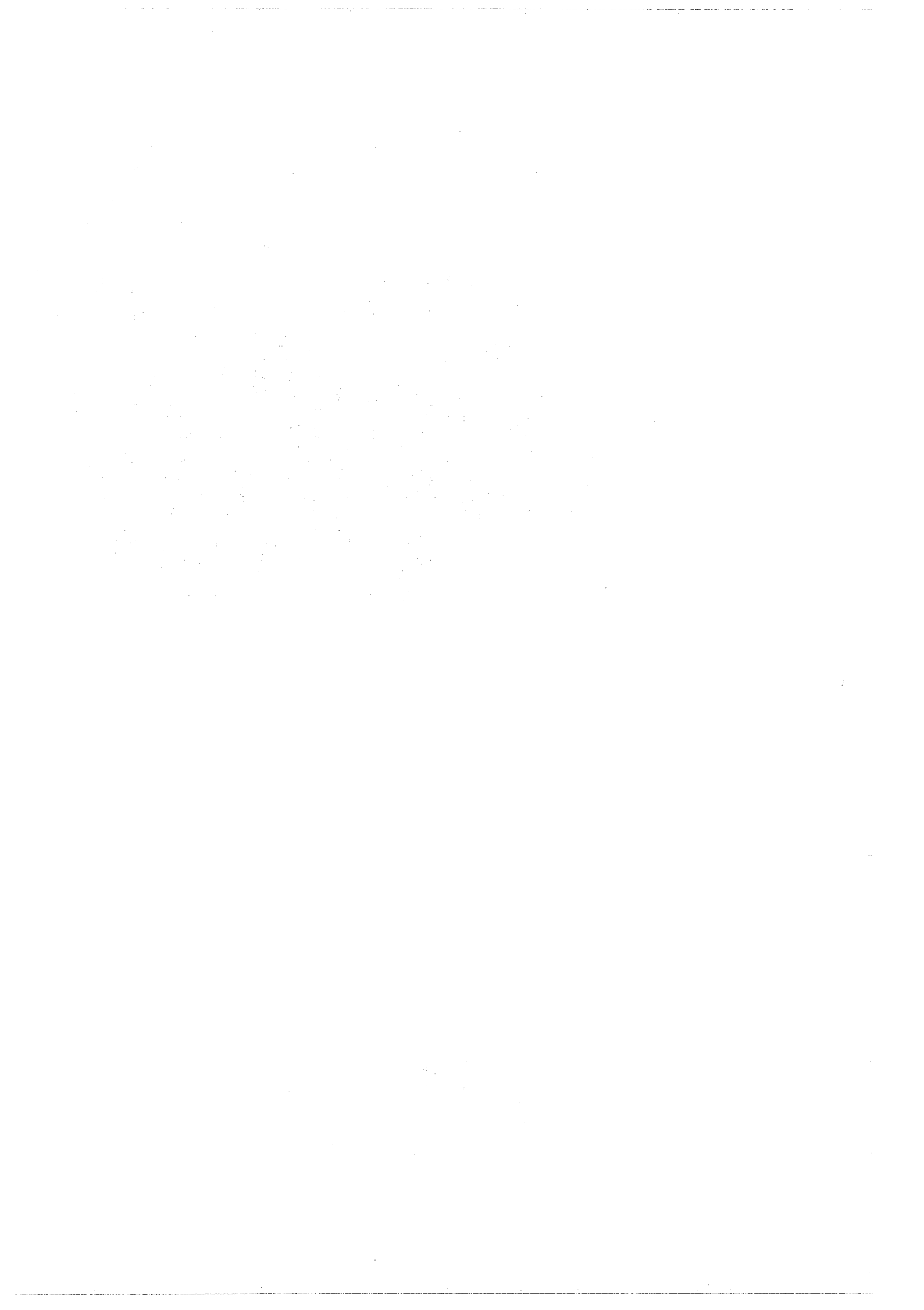
Institut für Reaktorbauelemente

Fuel Rod Bundles with Various Spacer Designs for  
Sodium Cooled Fast Reactors

W. Baumann, H. Hoffmann, R. Möller



GESELLSCHAFT FÜR KERNFORSCHUNG M. B. H.  
KARLSRUHE



KERNFORSCHUNGSZENTRUM KARLSRUHE

März 1970

KFK 1154

IAEA-SM-130/38

Institut für Reaktorbauelemente

Fuel Rod Bundles with Various Spacer Designs for  
Sodium Cooled Fast Reactors.

W. Baumann, H. Hoffmann, R. Möller

(Presented by H. Hoffmann)

Gesellschaft für Kernforschung mbH., Karlsruhe



Table of Contents:

Abstract

1. Introduction

2. Pressure-drop in Fuel Elements with  
Different Types of Spacers

3. Coolant Temperature Profile in the  
Outlet Cross Section of the Fuel Element  
as a Function of the Type of Spacer

4. Summary

Nomenclature

References

Tables and Illustrations

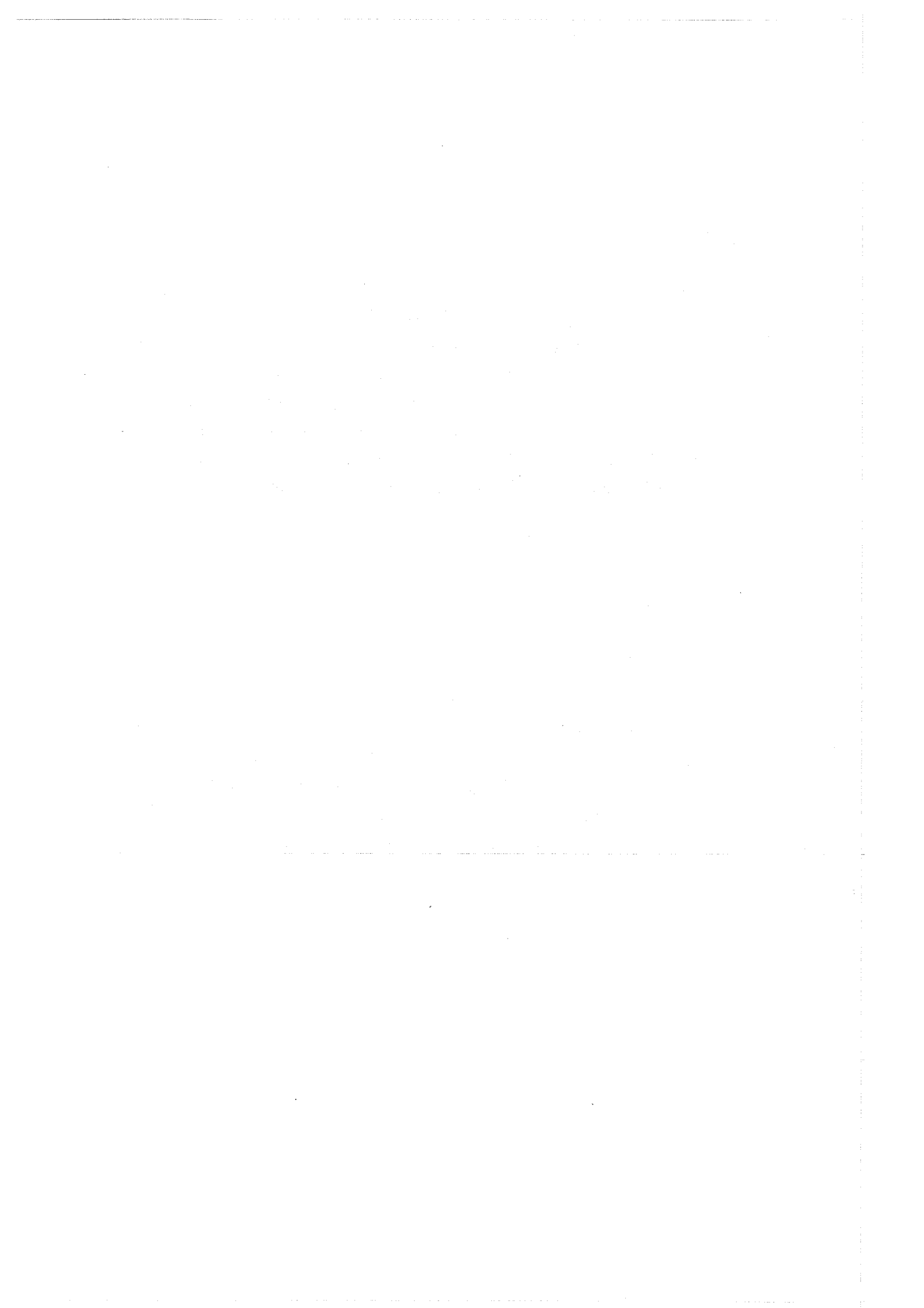


### Inhalt:

Der im Brennelement eines natriumgekühlten Schnellen Reaktors auftretende Druckverlust sowie das im Austrittsquerschnitt des Bündels zu erwartende Temperaturprofil werden als Funktion der Brennstabanordnung für gitter- und wendelförmige Abstandshaltertypen berechnet. Diese Betrachtungen stützen sich auf Ergebnisse aus experimentellen Untersuchungen des Druckverlustes und der Kühlmittelquervermischung ab.

### Abstract:

The pressure drop in a sodium cooled multirod fuel element and the temperature profile across its outlet section are calculated as a function of different rod arrays for grid- and helical-type spacers. These considerations are based on experimental pressure drop and coolant cross-mixing investigations.



## 1. Introduction

The pins of the fuel elements of fast reactors are combined in a bundle in a regular hexagonal array. The following spacers can be used to support the pins at different axial planes (Fig. 1):

Grid-type designs: honeycomb grids  
rhombus grids

Helical designs: 1 wire per rod  
1,3,6 helical fins per rod

Grid-type spacers and wires wrapped around the rods are separate components of the fuel element. In this case, the spacers are in direct contact with the thin wall of the cladding. Helical fins are an integral part of the cladding and can be manufactured in one procedure with the tube. Adjacent rods support each other via the top of the fins, so that the thin wall of the cladding is not touched by the spacer.

The evaluation and optimization of these spacers are determined mainly by their hydro-thermodynamical as well as mechanical-dynamical properties. They must be known as a function of the desired reactor operating conditions and the pitch-to-diameter ratio of the pins in the bundle.

These are the main requirements the spacers should fulfill:

- The pressure loss in the fuel element they help to create should be small in order to keep the coolant pumping capacity low.
- The local coolant temperatures they influence in the outlet cross section of the fuel element should be as uniform as possible and thus allow an optimum reactor power for a maximum permissible cladding temperature.

- The spacers should be economical in terms of fabrication, easy to assemble and dismantle and should guarantee failproof support of the pins throughout the operating life of the fuel element.

These aspects for the evaluation and selection of spacers were investigated. The preconditions were supplied by experiments in water, air, and sodium loops. The  $p/d$ -range considered  $1,17 \leq p/d \leq 1,32$  is limited by the design data for the BN-600 and the SNR-reactors [7,8]. The interesting Re-number region is  $5 \times 10^4 \leq Re \leq 1,5 \times 10^5$ .

## 2. Pressure-drop in Fuel Elements with Different Types of Spacers

The overall pressure-drop in a fuel element is composed of three fractions:

- Loss of pressure of the bundle without spacers
- Loss of pressure of the spacers
- Losses at bundle inlet and outlet.

For comparison of the pressure-drops of the spacers considered here the bundle inlet and outlet pressure-drops are insignificant because they occur to the same extents in each bundle.

The pressure-drops in the bundles without and with spacers are calculated from the equations listed in Table 1. For evaluation of these equations the friction factors  $\lambda_B$ ;  $\lambda_W$  and the loss-coefficient  $\xi$  must be known.

The friction factors of bundles without spacers are known from a multitude of theoretical and experimental investigations. The most important results [1,2,3,4,5] are summarized in Fig. 2. The curve represented is the friction-factor of the bundle related to that of the circular tube as a function of the pitch - to - diameter ratio of the rods  $p/d$ .

It is seen that the friction coefficients exceed that of the circular tube by 4 - 5 % in the  $p/d$ -range  $1.17 < p/d < 1.32$ .

Results from pressure-drop experiments with different lattice-type spacers [6] are shown as loss coefficient versus Re-number in Fig. 3. It is seen that the average modified loss coefficient for the interesting range of Re-numbers considered is

$$\xi_v = 6 - 7$$

The friction factors of bundle geometries with helical spacers [3] are listed in Fig. 4 as a function of the Re-number.

This provides the necessary data for a comparison of the pressure-drops of the different spacer types which is carried out for the following preconditions:

- Constant coolant mass flow through the bundle. The operating conditions of the reactor remain unchanged, i.e., with constant rod power there will be the same overall temperature increase of the coolant.
- The support-length of the pins in the bundle is fixed at  $l = 100$  mm.
- The calculations are based on the operating data and geometries indicated in Table 2.

A change of the operating data will have but a minor influence on the comparison of the pressure-drop results, because the Re-number changes only in a very small range and thus would hardly influence the pressure-drop coefficients. However, changes of the geometry of the bundles

and spacers (e.g., length of support, width of fins, wall-thickness of grids) have an effect upon the absolute level of the pressure-losses.

The result of the pressure-drop comparison is shown in Fig. 5. The plot indicates the loss of pressure per meter length of bundle as a function of the  $p/d$  ratio.

It can be seen:

- For a constant  $p/d$  ratio all spacers result in different pressure losses in the fuel element bundle which may differ by up to a factor of 2. The order of increasing pressure drops for the spacers considered here is this:

For  $p/d = 1.17$ :

1 helical fin  
1 helical wire  
3 helical fins  
6 helical fins  
Honeycomb grid

For  $p/d = 1.32$ :

3 helical fins  
1 helical fin  
Rhombus grid  
6 helical fins  
1 helical wire  
Honeycomb grid

- With increasing  $p/d$  ratio the pressure losses decrease very rapidly, e.g., by a factor of 3 between  $1.17 < p/d < 1.32$ .
- Some grid designs can be used only in specific  $p/d$  ranges, e.g., the rhombus grid for  $p/d > 1.23$ .
- The selection of suitable spacers cannot be made on the basis of pressure drop-comparison only, since some of the differences are very small indeed.

One exception is the honeycomb grid, which has by far the highest pressure loss for all  $p/\rho d$ -ratios.

The results of these calculations are summarized in Table 3, referred to the 3 finned tube bundle. This table also shows that reduced wall thicknesses of the grids or smaller fin widths are capable of greatly reducing the pressure-losses. Enlarged support lengths have practically no influence upon the pressure-drop of 3 and 6 finned tube bundles, but they do reduce it with the other types of spacers.

### 3. Coolant Temperature Profile in the Outlet Cross Section of the Fuel Element as a Function of the Type of Spacer

During reactor operation the maximum permissible cladding temperature must not be exceeded. With a given differential temperature between the heat releasing wall and the coolant the maximum permissible sodium temperature is thus fixed. This differential temperature depends on the spacer in two ways:

- The spacer determines the geometry of the flow channels in the bundle; in particular, it sets the distance between the peripheral pins and the wall of the fuel element box and hence the size of the cooling channels at the wall of the box. Since shape and dimensions of these subchannels differ from the inner channels of the bundle, the results are different flow conditions, coolant mass flows, and temperature increase of the coolant over the fuel element cross section.
  
- The existing connection of the fuel element subchannels permits a continuous exchange of mass and energy between hot channels and their environment,

which is called coolant cross mixing. This effect balances the differential temperatures of adjacent channels. The magnitude of exchange of mass and energy is determined by the geometry of the bundle and the type and arrangement of the spacers.

The temperature profiles in the outlet cross section of a fuel element were calculated for the types of spacers mentioned above under the operating conditions mentioned in table 2 and for the  $p/d$  range of interest, namely  $1.17 \leq p/d \leq 1.32$  [7,8]. The calculations were performed with the MISTRAL computer program [9]. The anticipated magnitudes of coolant cross mixing for the spacers included in the calculation were those values which had been determined experimentally in an air flow [10]. The thermal conduction of sodium as an exchange function between the subchannels of the bundle was taken into account in the calculations.

The deviations from the average coolant outlet temperature occurring in various subchannels of the bundle are indicated in Fig. 6 for  $p/d = 1.32$  and Fig. 7 for  $p/d = 1.17$ . It is seen that the wire-type spacer in the central part of the bundle attains the highest temperatures, although coolant cross mixing reaches peak values. This excess temperature reduces the safety margin to the maximum permissible cladding temperature. The use of a different type of spacer makes it possible either to increase this safety margin or to increase the coolant outlet temperature. This again allows an increase in reactor power or a reduction of coolant mass flow rate and, hence, a reduction of the pressure loss.

Decreasing the  $p/d$ -ratio from 1.32 to 1.17 results in a slightly increasing temperature of  $4^{\circ}$  C in the central part of the bundle. The spacers can be arranged in the order of increasing temperatures as follows:

3 fins per rod  
6 fins per rod / honeycomb grid  
rhombus grid ( $p/d = 1.32$ )  
1 wire / 1 fin per rod

These considerations apply to a 61-rod bundle. When changing to a 169 (469) rod bundle the excess temperatures are reduced to about 0.6 (0.35) of the values indicated here.

In order to confirm for sodium flows the assumptions about the magnitude of coolant cross mixing made from experiments in air, initial experiments have been carried out on a 61-rod bundle with SNR dimensions and grid-type spacers. The results of these investigations in sodium are shown in Fig. 8. They justify the assumptions made.

#### 4. Summary

It has been shown that fuel elements of tubes with integral helical fins as spacers generate balanced temperature profiles with low pressure loss. Last year, success has been achieved in the fabrication of these tubes to the dimensions and tolerances we desired and in largely developing the methods of tube testing. A 37-rod bundle of tubes with six integral helical fins was tested under conditions which exceeded those of sodium cooling [11]. This bundle, shown in Fig. 9, has proved the excellent mutual supporting action of the fuel pins by integral helical fins. A 61-rod bundle with the specific dimensions of SNR is being prepared for an experiment in a sodium flow.

Nomenclature:

b	width of the fin
d	rod diameter
$d_h$	hydraulic diameter
F	flow area
$F_v$	projection area of grids
L	length
l	support length
$\dot{m}$	mass flow rate
n	number of rods per bundle
p	rod pitch
$\Delta p$	pressure drop
Re	Reynolds-number
r	radial coordinate
s	thickness of web plate
t	temperature
w	velocity
z	number of grids per bundle
$\xi$	loss coefficient of grid type spacers
$\xi_v$	$\frac{\xi}{(F_v/F_B)^2}$ modified loss coefficient of grid type spacers
$\Delta t$	$t_{out} - (t_{out})_m$
$\lambda$	friction factor
$\mu$	<u>cross mass flow per unit axial length</u> total mass flow in a subchannel
$\rho$	density
$\chi$	rod power
$\varphi$	flux factor

Subscripts:

B Bundle

G grid

m mean

out outlet

R smooth tube

W wire wrap

## References:

- [1] EIFLER, W., NIJSING, R.; 'Experimental investigation of velocity distribution and flow resistance in a triangular array of parallel rods.' Nuclear Engineering and Design 5, 1967
- [2] SUBBOTIN, V.I., et. al.; 'Hydraulic resistance to the flow of a liquid along a bundle of rods.' Sov. J. Atom. Energy 9, 1961
- [3] BAUMANN, W., CASAL, V., HOFFMANN, H., MÖLLER, R., RUST, K.; 'Brennelemente mit wendelförmigen Abstandshaltern für Schnelle Brutreaktoren.' KFK 768, EUR 3694 d, April 1968
- [4] DEISLER, R.G., TAYLOR, M.T.; 'Analysis of Axial Turbulent Flow and Heat Transfer Through Banks of Rods and Tubes.' TID 7529, 1957
- [5] GALLOWAY, L.R., Epstein, N.; 'Longitudinal flow between cylinders in square and triangular arrays and in a tube with square-edged entrance.' AIChE-1 Chem. E. Symposium Series No. 6, 3-15 (1965)
- [6] REHME, K.; 'Widerstandsbeiwerte von Gitterabstandshaltern für Reaktor-Brennelemente.' Atomkernenergie (im Druck)
- [7] LEIPUNSKII, A.J., et. al.; 'The BN-600 Fast Reactor' Technical Meeting Nr. 4/5, Nuclex 69, 6.-11. Okt.1969
- [8] GAST, K., SCHLECHTENDAHL, E.G.; 'Schneller Natriumgekühlter Reaktor Na-2.' KFK 660, EUR 3706 d, Oktober 1967

- [9] BAUMANN, W.; 'MISTRAL - Thermodynamischer Mischströmungsalgorithmus für Stabbündel (16740):  
- ein digitales Rechenprogramm zur Ermittlung örtlicher Temperaturen und Massenströme in 61-Stabbündeln unter Berücksichtigung der Kühlmittel-Quervermischung und des Energieaustausches durch Wärmeleitung -.' KFK 988, Juni 1969
- [10] BAUMANN, W., MÖLLER, R.; 'Experimental study of Coolant Cross-Mixing in multirod bundles, consisting of unfinned, one-, three- and six-fin rods.  
Atomkernenergie 14-5 ; 1969
- [11] HOFFMANN, H., HOFMANN, G., LEISTIKOW, S.; 'Experimentelle Untersuchungen des Druckverlustes des Langzeitverhaltens der Abstützstellen an einem Modell-Brennelement aus Incoloy 800-Rohren mit sechs integralen Wendelrippen als Abstandshalter in einer isothermen Heißdampfströmung.' KFK 1028, EUR 4304 d, Sept. 1969
- [12] SCHLICHTING, H.; 'Grenzschicht-Theorie.' Verlag G.Braun Karlsruhe, 5. Aufl., 1964

Bundle without spacers:

$$\Delta p_B = \lambda_B \cdot \frac{L}{d_h} \cdot \frac{\rho w^2}{2}$$

Bundle with grid-type spacers:

$$\Delta p_{BG} = (\lambda_B \cdot \frac{L}{d_h} + z \xi) \cdot \frac{\rho w^2}{2}$$

where  $\xi = \xi_V \cdot \left(\frac{F_V}{F_B}\right)^2$

Bundle with helical spacers:

$$\Delta p_W = \lambda_W \cdot \frac{L}{d_h} \cdot \frac{\rho w^2}{2}$$

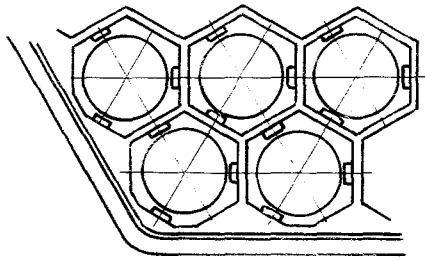
Table 1: Equations for pressure-drop calculations in bundles with different types of spacers

Core inlet temperature	$t_1 = 380^\circ \text{ C}$
Core outlet temperature	$t_w = 560^\circ \text{ C}$
Maximum rod power	$\chi_{\text{max}} = 400 \text{ W/cm}$
Axial flux factor	$\varphi_{\text{ax}} = 0.78$
Pin diameter	$d = 6 \text{ mm}$
Number of rods per bundle:	$n = 169$
Length of bundle:	$L = 1 \text{ m}$
Length of support:	$l = 100 \text{ mm}$
Fin geometry:	
Width	0.6 mm
Height for 3/6 fins	$(p-d)/2$
for 1 fin	$p-d$
Wire geometry:	
Diameter	$p-d$
Thickness of web plates of the grids	0.4 mm

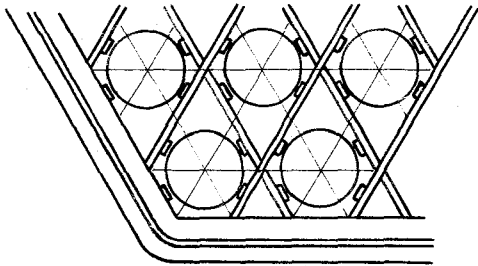
Table 2: Operating Data and Geometries for the Calculations of Pressure-loss and Temperature Profile.

Support-length l (mm)	100			150			200		
Pitch to diameter ratio p/d	1.167	1.25	1.317	1.167	1.25	1.317	1.167	1.25	1.317
Type of spacer									
1 helical wire	0.90	1.16	1.53	0.75	0.86	1.00	0.69	0.78	0.91
1 helical fin b=0.6	0.85	0.98	1.17	0.71	0.72	0.76	0.65	0.66	0.70
3 helical fins	b=0.6	1.00	1.00	1.00	1.00	1.00	1.00	1.00	1.00
	b=0.4	0.94	0.94	0.94	0.94	0.94	0.94	0.94	0.94
6 helical fins	b=0.6	1.22	1.30	1.35	1.22	1.30	1.35	1.22	1.30
	b=0.4	1.09	1.13	1.17	1.09	1.13	1.17	1.09	1.13
Rhombus grid	s=0.4	-	1.22	1.26	-	0.98	1.00	-	0.85
	s=0.3	-	1.03	1.10	-	0.85	0.90	-	0.76
Honeycomb grid	s=0.4	1.69	1.95	2.22	1.33	1.50	1.67	1.15	1.26
	s=0.3	1.33	1.58	1.86	1.09	1.25	1.43	0.97	1.08

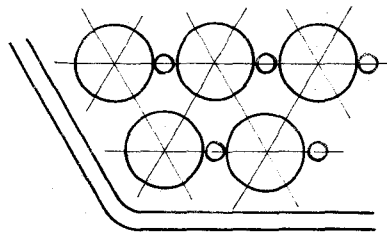
Table 3: Normalized pressure losses for bundles with different types of spacers, referred to the bundle with three helical fins per rod and as a function of the support length as well as the pitch to ratio p/d of the rods.  
Precondition: Constant mass flow rate.



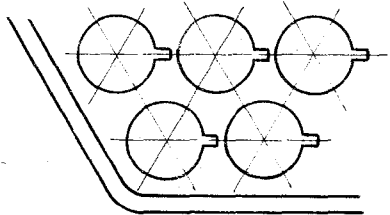
- honeycomb grid



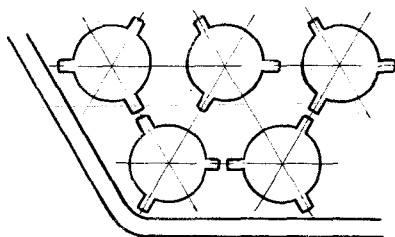
- rhombus grid



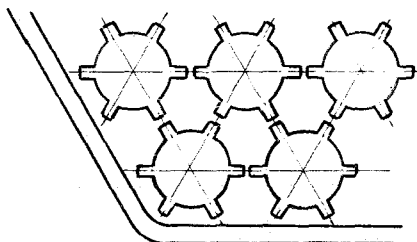
- wire wrapped rods



- 1-fin tubes



- 3-fin tubes



- 6-fin tubes

Fig. 1: Different Spacers for the Fuel Elements of Sodium Cooled Fast Breeder Reactors.

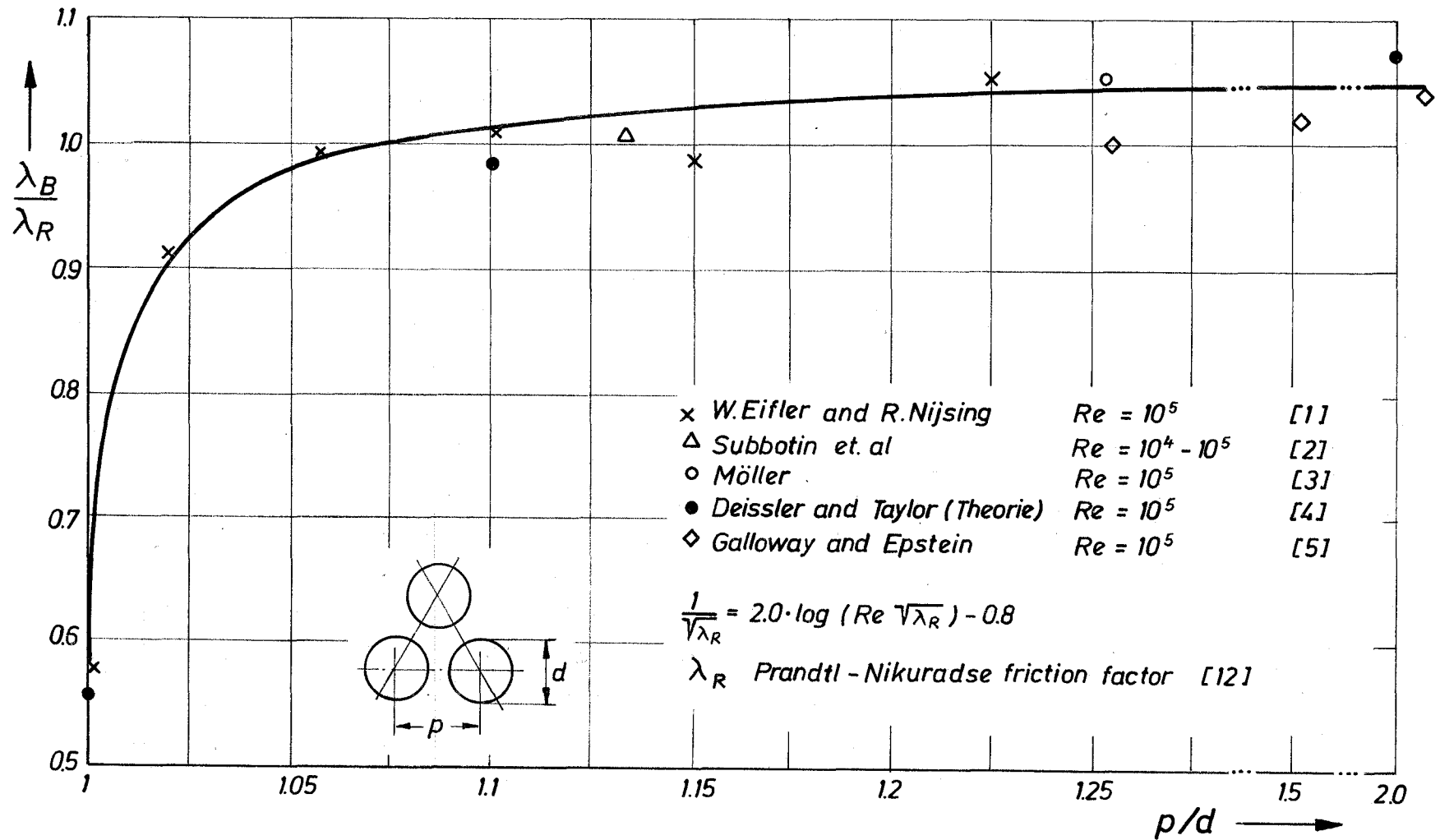


Fig. 2: Relative Friction Factor for Hexagonally Arranged Rod Clusters as a Function of the  $p/d$  - Ratio.

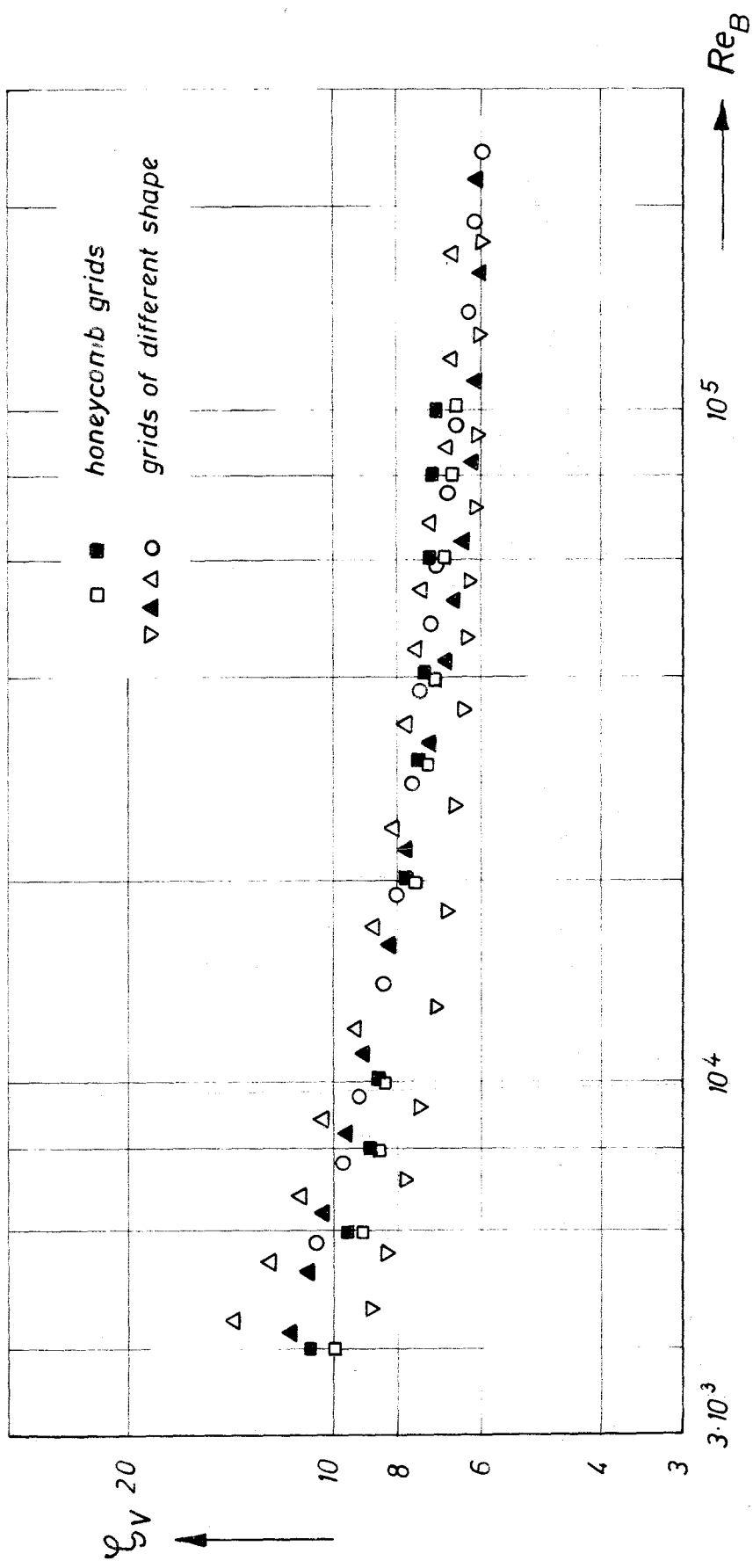


Fig. 3: Modified Loss Coefficient  $\zeta_v$  as a Function of the Reynolds - Number [67]

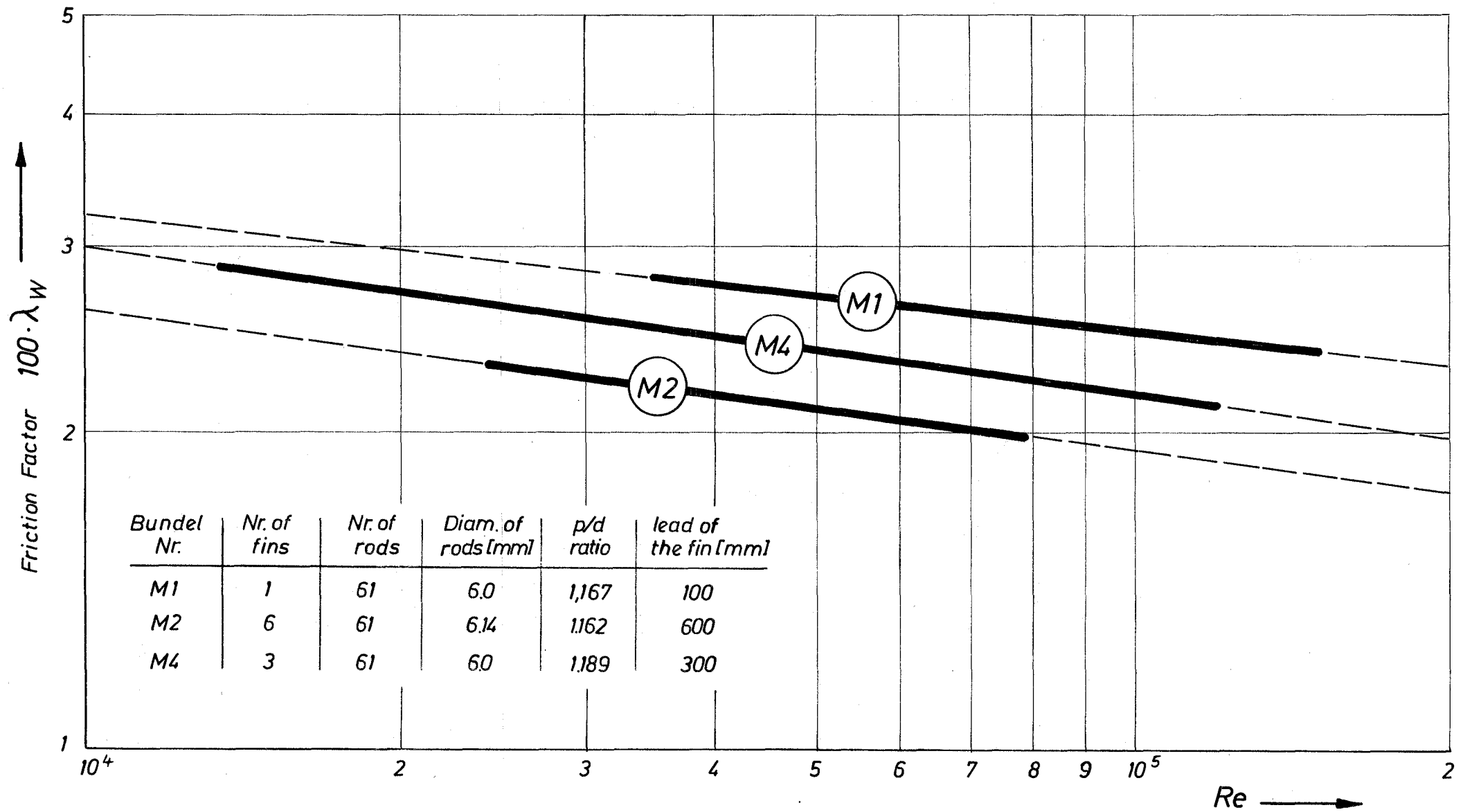


Abb. 4: Friction Factor as a Function of the Reynolds - Number for Rod Bundles with Helicaltype Spacers.

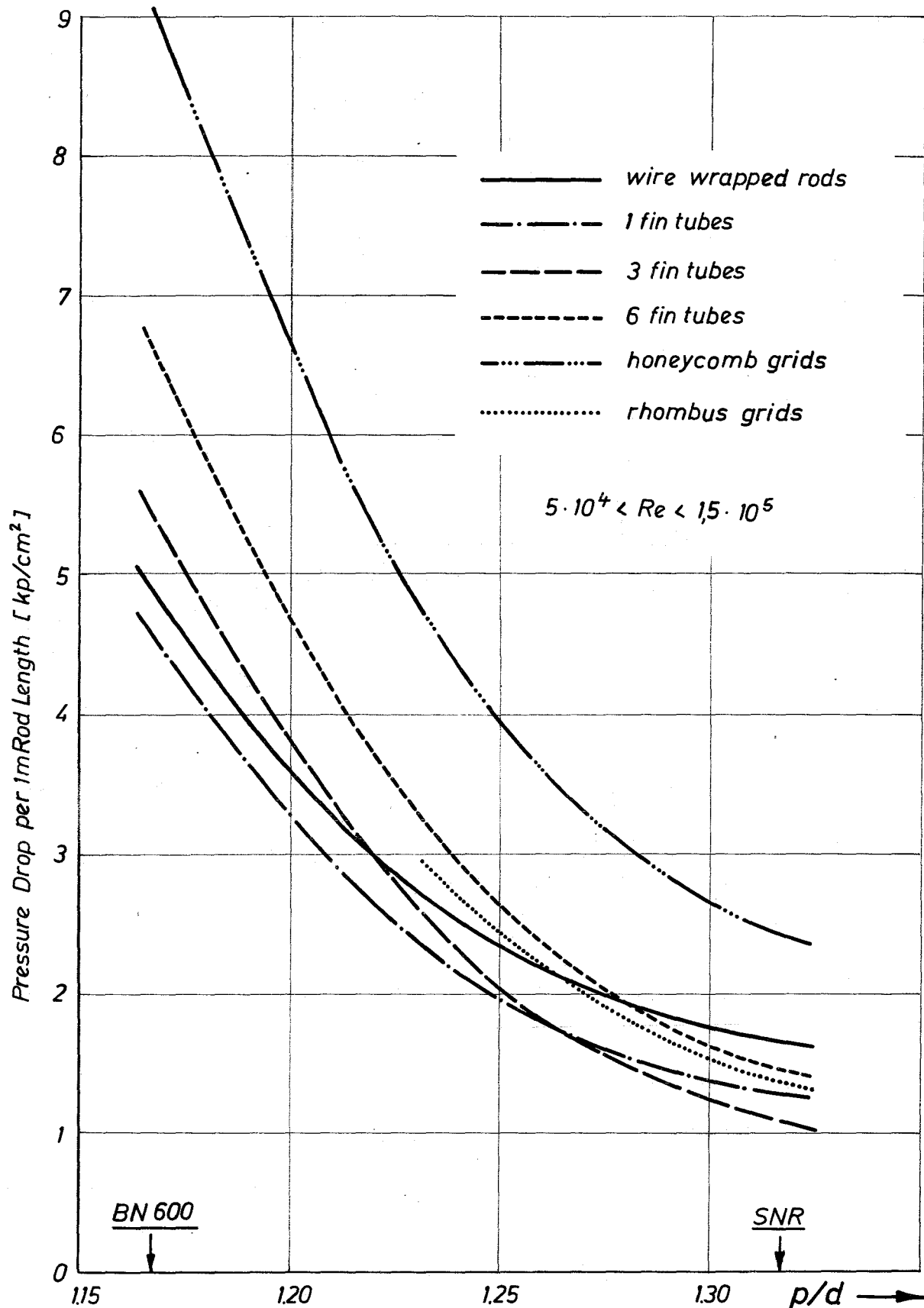


Fig. 5: Pressure Drop in Rod Bundles with Different Spacers as a Function of the  $p/d$ -Ratio.

Support Length:  $l = 100 \text{ mm}$   
 Rod - Diameter:  $d = 6 \text{ mm}$   
 Number of Rods:  $n = 169$   
 Mass Flow Rate:  $\dot{m} = \text{constant}$

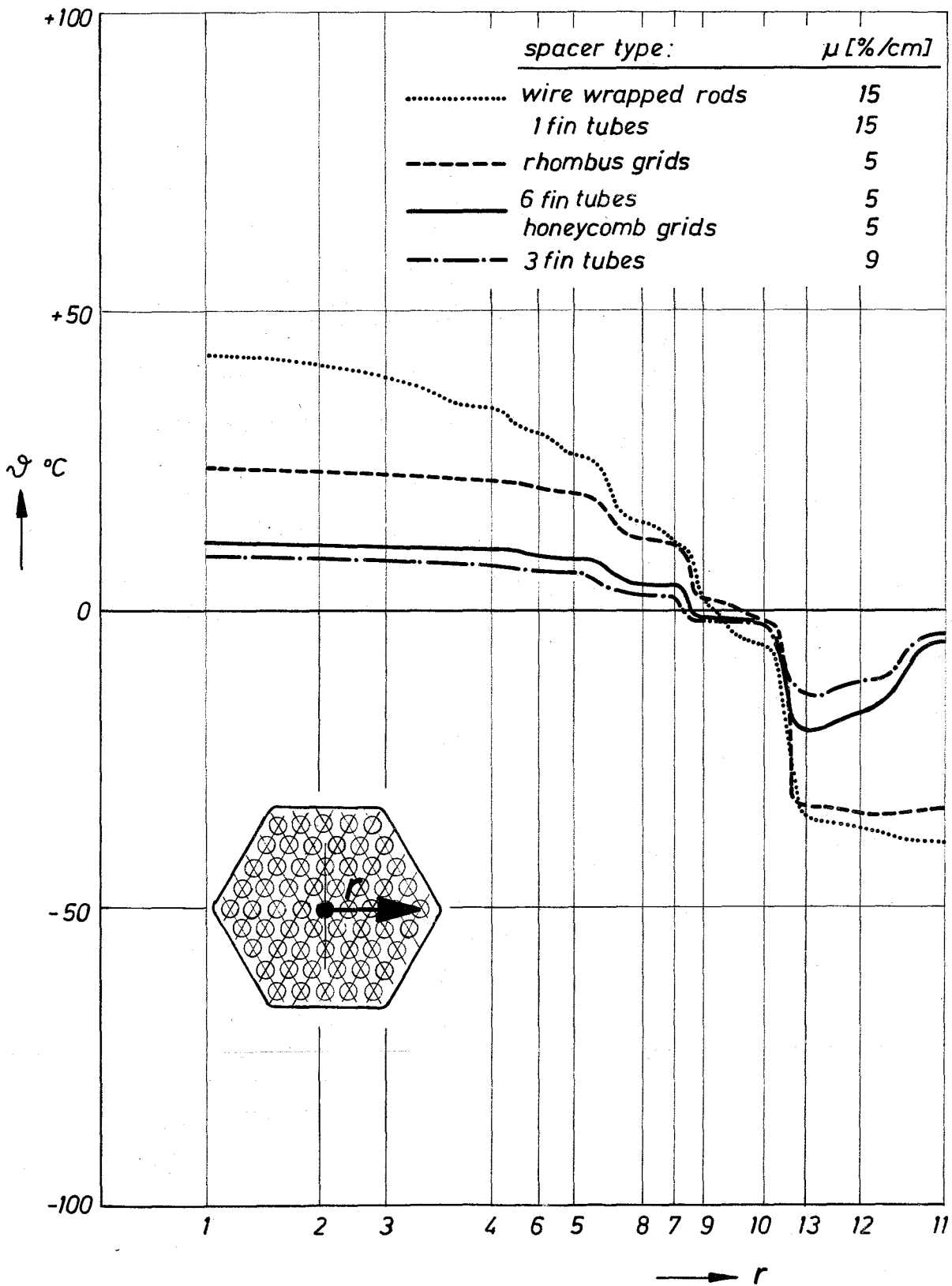


Fig. 6 Coolant Outlet -Temperature Profiles  $\Delta t = t_{out} - (t_{out})_m$  for Different Spacers as a Function of Radial Subchannel Position and Coolant Cross Mixing  $\mu$  [%/cm];  $l = 100$  mm;  $p/d = 1,32$

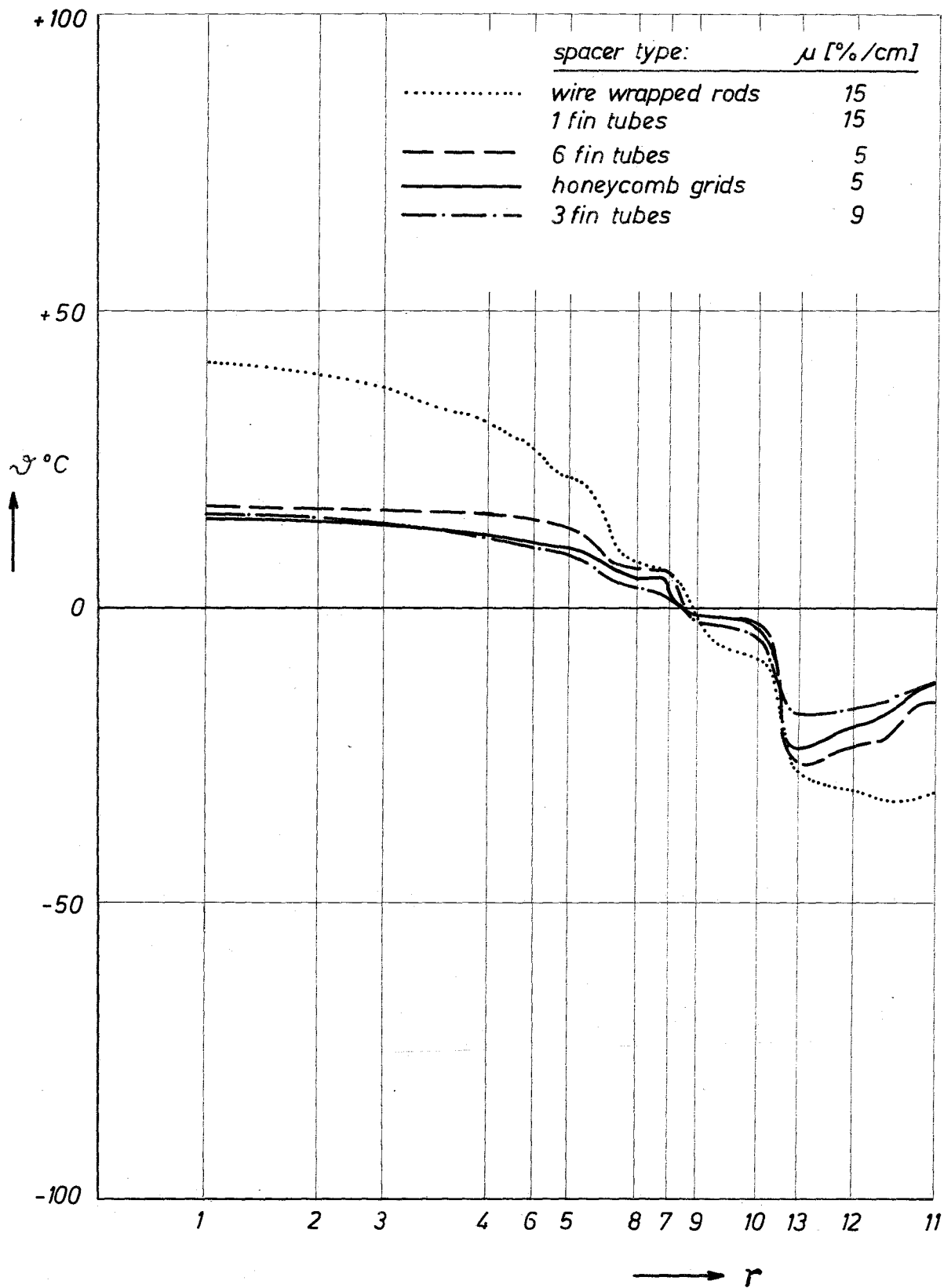


Fig. 7 Coolant Outlet-Temperature Profiles  $\vartheta = t_{out} - (t_{out})_m$  for Different Spacers as a Function of Radial Subchannel Position and Coolant Cross Mixing  $\mu$  [%/cm];  $l = 100$  mm;  $p/d = 1.17$

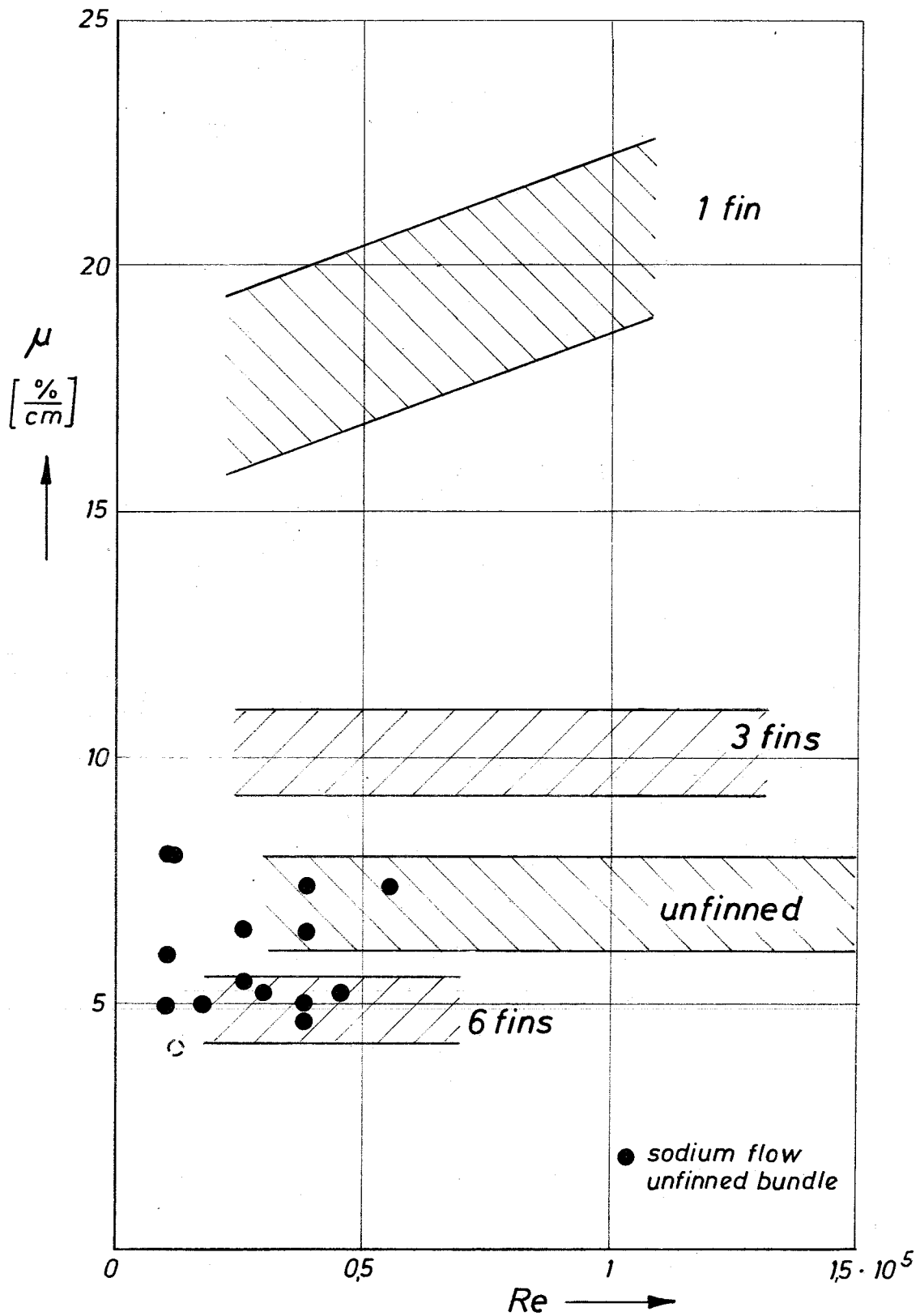
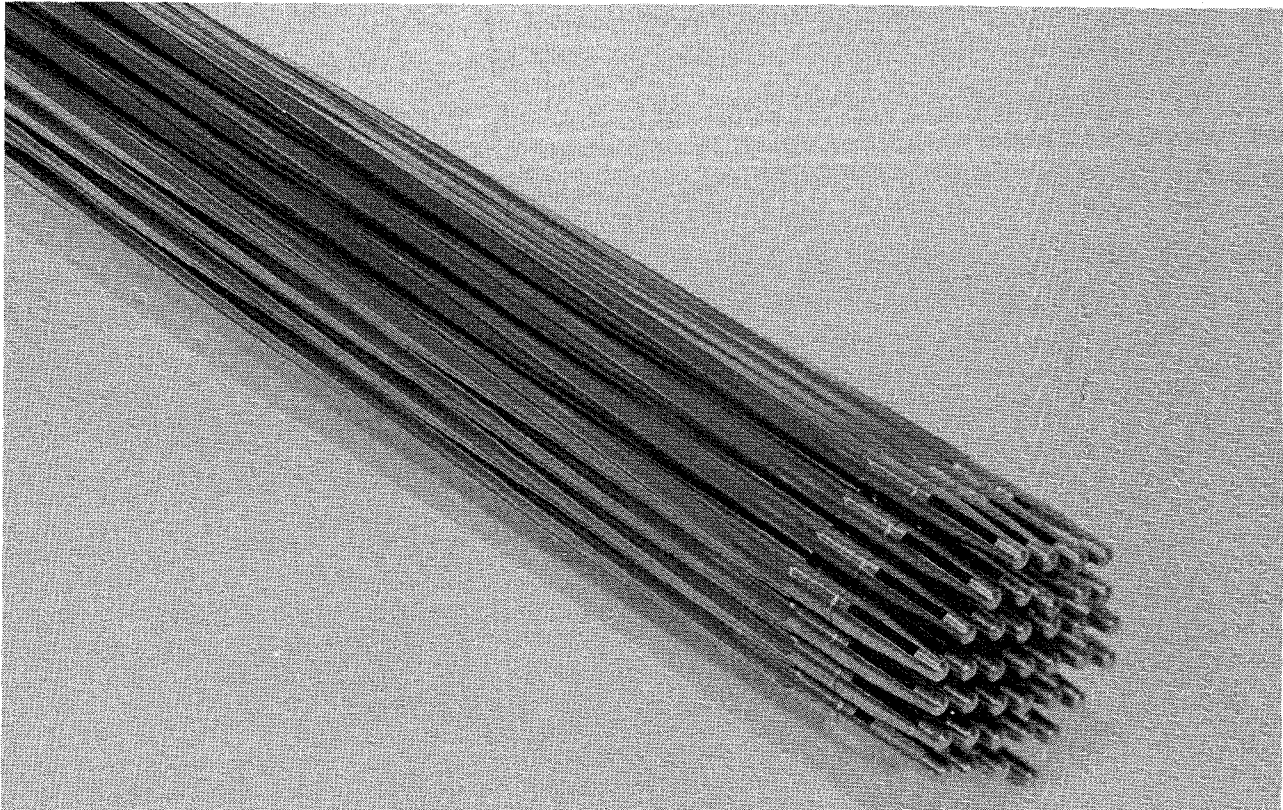
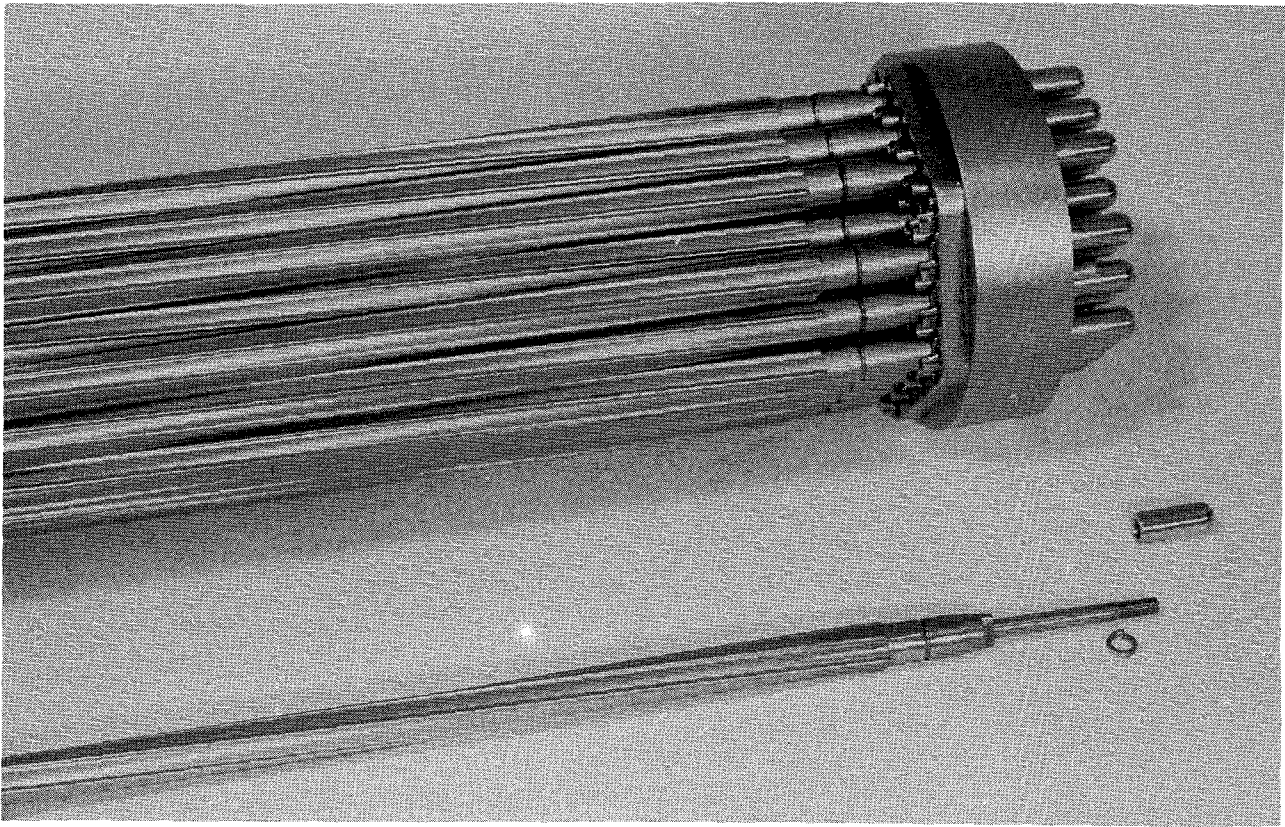


Fig. 8 Mixing Rate  $\mu$  as a Function of the Reynolds-Number for Fuel-Elements with Finned and Unfinned Rods.



*Fig. 9 Bundle of Rods with 6 Integral Helical Fins as Spacers. Lower and Upper End of the Subassembly.*

